January 1998 • NREL/SR-520-23994

Polycrystalline Thin-Film Cadmium Telluride Solar Cells Fabricated by Electrodeposition

Annual Technical Report

J.U. Trefny and D. Mao
Department of Physics
Colorado School of Mines
Golden, Colorado

National Renewable Energy Laboratory
1617 Cole Boulevard
Golden, Colorado 80401-3393
A national laboratory of
the U.S. Department of Energy
Managed by Midwest Research Institute
for the U.S. Department of Energy
under Contract No. DE-AC36-83CH10093

NREL/SR-520-23994 • UC Category: 1263

Polycrystalline Thin-Film Cadmium Telluride Solar Cells Fabricated by Electrodeposition

Annual Technical Report

J.U. Trefny and D. Mao
Department of Physics
Colorado School of Mines
Golden, Colorado

NREL technical monitor: B. von Roedern

National Renewable Energy Laboratory
1617 Cole Boulevard
Golden, Colorado 80401-3393
A national laboratory of
the U.S. Department of Energy
Managed by Midwest Research Institute
for the U.S. Department of Energy
under Contract No. DE-AC36-83CH10093

Prepared under Subcontract No. XAF-5-14142-11
January 1998

NOTICE

This report was prepared as an account of work sponsored by the National Renewable Energy Laboratory, managed by Midwest Research Institute, in support of its Subcontract No. XAF-5-14142-11 with Colorado School of Mines. Neither the National Renewable Energy Laboratory, nor the Midwest Research Institute, nor Colorado School of Mines, nor any of their employees, nor any of their contractors, nor any of their subcontractors, nor any of their employees, makes any warranty, express or implied, or assumes any legal liability or responsibility for the accuracy, completeness or usefulness of any information, apparatus, product or process disclosed, or represents that its use would not infringe privately owned rights.

This publication was reproduced from the best available camera-ready copy submitted by the subcontractor and received no editorial review at NREL.

NOTICE

Available to DOE and DOE contractors from:
Office of Scientific and Technical Information (OSTI)
P.O. Box 62
Oak Ridge, TN 37831
Prices available by calling (423) 576-8401

Available to the public from:
National Technical Information Service (NTIS)
U.S. Department of Commerce
5285 Port Royal Road
Springfield, VA 22161
(703) 487-4650

Executive Summary

Objectives

The objective of this project is to develop improved processes for the fabrication of CdTe/CdS polycrystalline thin film solar cells. The technique we use for the formation of CdTe, electrodeposition, is a non-vacuum, low-cost technique that is attractive for economic, large-scale production.

Technical Approach

During the past year, our research and development efforts have focused on several steps that are critical to the fabrication of high-efficiency CdTe solar cells.These include the study of growth and properties of electrodeposition CdS, quantitative studies of CdTe-CdS interdiffusion using x-ray diffraction and photoluminescence, and back contact formation using Cu-doped ZnTe with an emphasis on low Cu concentrations. We have also started to explore the stability of our ZnTe-Cu contacted CdTe solar cells.

Results

Studies of the growth and properties of electrodeposited CdS thin films.

Uniform, high-quality CdS thin films are highly desirable for the fabrication of high-efficiency CdTe/CdS solar cells. Currently, chemical bath deposition is the most successful among all techniques. Other techniques, such as vacuum sublimation, have been used. However, because of a higher density of pinholes in the deposited films, the minimum CdS thickness required for obtaining high V_{oc} is much greater than for CBD CdS. Electrodeposition is a non-vacuum technique and is compatible with our CdTe deposition process. Moreover, it offers excellent control over the properties of the thin films through the influence of deposition potential, bath temperature, pH, and composition of reactants. We have investigated the electrodeposition of CdS and its application in fabricating CdTe/CdS solar cells. The electrodeposition of CdS was done in a system that consisted of a glassy-carbon anode, a Ag/AgCl reference electrode, and a cathode (sample substrate). The experimental conditions we explored in this study were: pH from 2.0 to 3.0; temperatures of 80° and 90°C; $CdCl_2$ concentration of 0.2 M; deposition potential from -550 to -600 mV vs. Ag/AgCl electrode; [$Na_2S_2O_3$] concentration between 0.005 and 0.05 M.

The electrodeposition rate of CdS was studied as a function of the solution temperature, sodium thiosulfate concentration, pH, and the acid used. The deposition rate increases with increase of the thiosulfate concentration and decrease of solution pH. Such a dependence can be understood based on the known disproportion of thiosulfate ions. With decreasing pH and increasing thiosulfate concentration, the disproportion rate increases, leading to increased deposition rate of CdS on the electrode. The high deposition rate observed at high solution temperature may be caused by both an increased reaction rate at the electrode and the increased thiosulfate disproportion rate. We also observed that the acid used to adjust the pH has a large impact on the deposition rate. The deposition is faster in a hydrochloric acid solution than in a sulfuric acid solution. The Faradaic efficiency of the electrodeposition process was calculated. The Faradaic efficiency is lower at low pH, caused presumably by the hydrogen evolution at low pH which contributes to the reduction current. In all

cases, the Faradaic efficiency was much lower than unity.

The surface morphology of electrodeposited CdS thin films was investigated using scanning electron microscopy. The most pronounced difference in film morphology was observed for different solution temperatures. Films deposited in a hydrochloric acid solution at 80°C consist of agglomerates of small crystallites. These agglomerates have a rather uniform size of ~0.7 μm and cover the tin oxide substrates uniformly. Films deposited at a higher temperature of 90°C are nonuniform with μm-size CdS agglomerates covering only a small portion of the substrates. Therefore, in terms of film uniformity and cell fabrication, deposition in a hydrochloric acid solution at 80°C is preferred. The improved uniformity can be related to the slow growth rate obtained under such conditions. The composition of the electrodeposited CdS was analyzed using Auger electron spectroscopy. The ratio of Cd and S concentrations is close to the stoichiometric value for films deposited at pH of 3.0. At lower pH, the films are more Cd rich. We have prepared CdTe/CdS cells using electrodeposited and physical vapor deposited CdTe on electrodeposited CdS. Moderate cell efficiencies were obtained in the preliminary study.

Studies of Cu-doped ZnTe back contact layer

The formation of stable, low-resistance back contacts to polycrystalline CdTe is a critical step in development of high efficiency CdTe thin film solar cells. One back contact material, Cu-doped ZnTe, has yielded very low contact resistance (<0.1 ohm.cm^2) and high fill factors (>0.74) in CdTe solar cells [1, 2]. Because of the high diffusivity of Cu in polycrystalline thin films, it is desirable to bring the Cu doping concentration to as low a level as possible while still maintaining the performance of the contact. We have extended our previous research on ZnTe:Cu films by investigating films doped with low Cu concentrations (<5.0 at. %). The low Cu concentration enabled us to increase the ZnTe:Cu post-deposition annealing temperature without causing excessive Cu diffusion into CdTe or formation of secondary phases. The effects of low Cu doping level and high temperature annealing on the stability of the CdS/CdTe/ZnTe devices were also investigated.

The effects of Cu doping concentration and post-deposition annealing temperature on the structural, compositional, and electrical properties of ZnTe were studied systematically using x-ray diffraction (XRD), atomic force microscopy (AFM), electron microprobe, Hall effect and conductivity measurements. XRD measurements indicated that the crystalline phase of as-deposited and low-temperature annealed ZnTe films is dependent on Cu doping concentration. Low-Cu-doped films exhibited zincblend phase, whereas high-Cu-doped films showed wurzite phase. After annealing at high temperature ($\geq$ 350°C), all films exhibited zincblende structure. Electron probe microanalysis revealed a deficiency of cations in low-Cu-doped films and excess of cations in high-Cu-doped films. Hall effect measurements revealed a dependence of hole mobility on Cu doping concentration with the highest mobility (20 cm^2/Vs) obtained at a low Cu concentration. Carrier concentrations higher than mid-10^{18}cm^{-3} were obtained at a Cu concentration of 2 at. % and relatively low annealing temperatures. Studies of the activation energy of dark conductivity suggested that intrinsic defects (e.g., Zn vacancies) are dominant acceptors for Cu concentrations lower than 4.5 at. %. Finally, ZnTe films with Cu concentrations as low as 1 at. % were used successfully as a back contact layer in CdTe based solar cells. Fill factors over 0.70 were obtained using ZnTe films of low Cu doping.

Table of Contents

List of Figures

List of Tables

1. Introduction

1.1 Background

Polycrystalline thin-film CdTe has attracted a great deal of interest for low-cost, high-efficiency photovoltaic energy conversion applications. Among the various techniques that are available for CdTe thin film deposition, electrodeposition is a non-vacuum technique and has the advantage of low cost, efficient utilization of raw material, and scalability for high-volume production. The objective of the CSM contract was to improve certain processing steps of the cell fabrication and to further our knowledge of the polycrystalline thin film materials. Improved efficiencies, high-quality film growth techniques, materials analysis, device fabrication and characterization have all been of particular interest in our work.

1.2 Cell Fabrication Procedure

The solar cell structure we investigate has a CdTe/CdS/SnO_2/glass structure. The standard cell fabrication procedure includes:

(1) Preparation of CdS thin films (typical thickness of 0.2 μm) by chemical bath deposition (CBD) or electrodeposition. CBD was performed in an alkaline solution containing cadmium acetate, ammonium acetate, ammonium hydroxide, and thiourea. Electrodeposition was done in an acidic solution containing $CdCl_2$ and $Na_2S_2O_3$.

(2) Annealing of the CdS films at 450°C for 50 min in a N_2 atmosphere. A $CdCl_2$ coating was applied to the CdS surface prior to annealing, using a mist generator containing a 1.2 M $CdCl_2$ aqueous solution.

(3) The electrodeposition of CdTe (typical thickness of 2 - 3.5 μm) using a system comprised of four electrodes: Cd and Te anodes, a Ag/AgCl reference electrode, and a cathode (sample substrate). The typical electroplating conditions were: pH, 2; temperature, 80°C; 1.2 M $CdCl_2$; deposition current between 0.26 and 0.40 mA/cm^2; deposition potential, -600 mV (vs. Ag/AgCl electrode); and anode current ratio close to 2.0.

(4) Annealing of CdTe/CdS films at 410°C for 40 min in dry air. Prior to annealing, a $CdCl_2$ coating was applied to the CdTe surfaces using the same procedure as used for the CdS layers.

(5) Etching of the CdTe surface in a 0.1% Br-MeOH solution for 10 s.

(6) Deposition of ZnTe films doped with Cu by vacuum evaporation. Cu concentration was varied between 1 and 8 at. %. The ZnTe:Cu layer thickness was varied from 40 to 150 nm.

(7) Post-deposition annealing in a N_2 environment in the temperature range of 170 to 280°C.

(8) Metal evaporation.

A wide variety of thin film and device characterization techniques were used to characterize our material. X-ray diffraction (XRD) measurements were performed on a Rigaku x-ray diffractometer using Cu-Kα radiation. Scanning electron microscopy (SEM) measurements were performed using a JOEL Model 840 instrument. Optical transmission and reflection measurements were performed using a CARY 5E UV-VIS-NIR spectrophotometer equipped with a PTFE integrating sphere. The finished cells were characterized using current-voltage, capacitance-voltage, and spectral response techniques.

2. Electrodeposited CdS Thin Films and Their Application in CdS/CdTe Solar Cells

We have investigated the electrodeposition of CdS and its application in fabricating CdTe/CdS solar cells. CdS is commonly used as an n-type window layer in CdTe solar cells. So far, chemical bath deposition (CBD) has been the most widely used technique for producing high efficiency devices because uniform, adherent, and conformal coatings can be obtained reproducibly using a simple technique. However, CBD has the disadvantage of low materials utilization and high volume waste production. For vacuum-based CdTe deposition technologies, the CBD of CdS is also incompatible with the CdTe deposition process. As such, other techniques have been studied to produce CdS films of comparable quality.

The electrodeposition of CdS was done in a system that consisted of a glassy-carbon anode, a Ag/AgCl reference electrode, and a cathode (sample substrate). The experimental conditions used in our study were: pH from 2.0 to 3.0; temperatures of 80° and 90°C; $CdCl_2$ concentration of 0.2 M; deposition potential from -550 to -600 mV vs. Ag/AgCl electrode; [$Na_2S_2O_3$] concentration between 0.005 and 0.05 M. Either HCl or H_2SO_4 was used for adjusting the pH. Typically, a film of 200 nm thick can be grown in less than 1 hr. The films exhibit a yellow color typical of pure CdS, in contrast with the orange color commonly shown by chemical bath deposited CdS.

Electrodeposition Process

The electrodeposition rate of CdS was studied as a function of the solution temperature, sodium thiosulfate concentration, pH, and the acid used. The deposition time required for the passage of 0.16 Coul/cm^2 charge, which is inversely proportional to the deposition rate, is plotted as a function of these deposition parameters (Figures 1-3). The deposition rate increases with increase of the thiosulfate concentration and decrease of solution pH (Figures 1 and 2). This dependence can be understood based on the known disproportion of thiosulfate ions:

$$S_2O_3^{2-} \rightleftharpoons S + SO_3^{2-}$$

and the overall electrode reaction:

$$Cd^{2+} + S_2O_3^{2-} + 2e^- \rightleftharpoons CdS + SO_3^{2-}$$

With decreasing pH and increasing thiosulfate concentration, the disproportion rate increases, leading to increased deposition rate of CdS on the electrode. The high deposition rate observed at high solution temperature may be caused by both an increased reaction rate at the electrode and the increased thiosulfate disproportion rate. We also observed that the acid used to adjust the pH has a large impact on the deposition rate. The deposition is faster in a hydrochloric solution than in a sulfuric acid solution (Figure 3).

The Faradaic efficiency of the electrodeposition process was calculated using the formula:

$$\text{Faradaic efficiency} = 3.22 \times 10^{-6} \text{ thickness (nm)} / \text{charge per unit area}$$

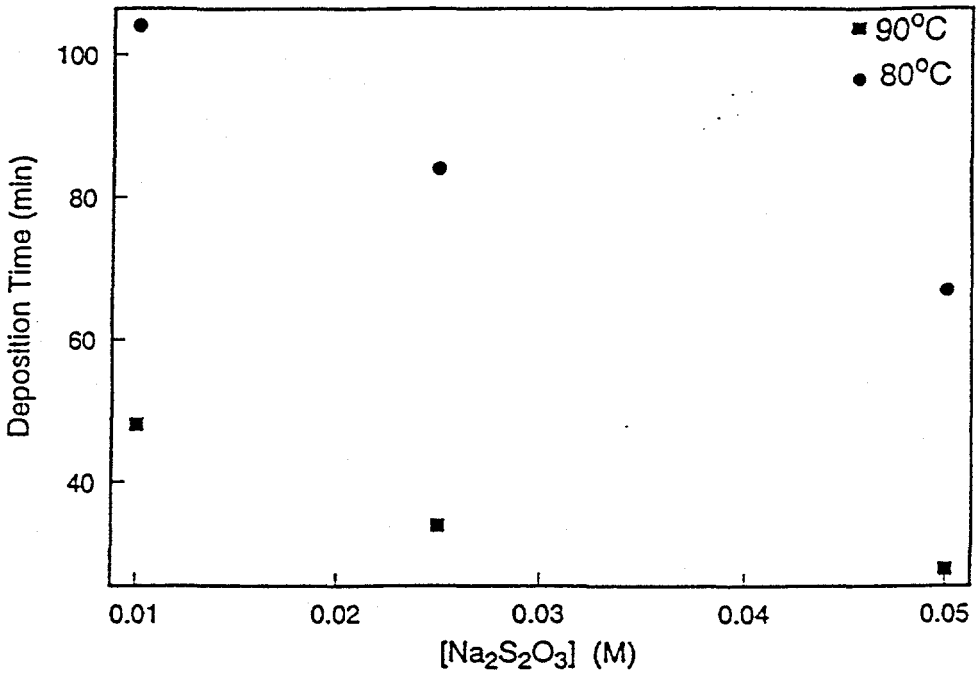

Figure 1. The deposition time required for the passage of 0.16 Coul/cm² charge as a function of the sodium thiosulfate concentration and solution temperature. The solution pH was 3.0. The acid used was HCl.

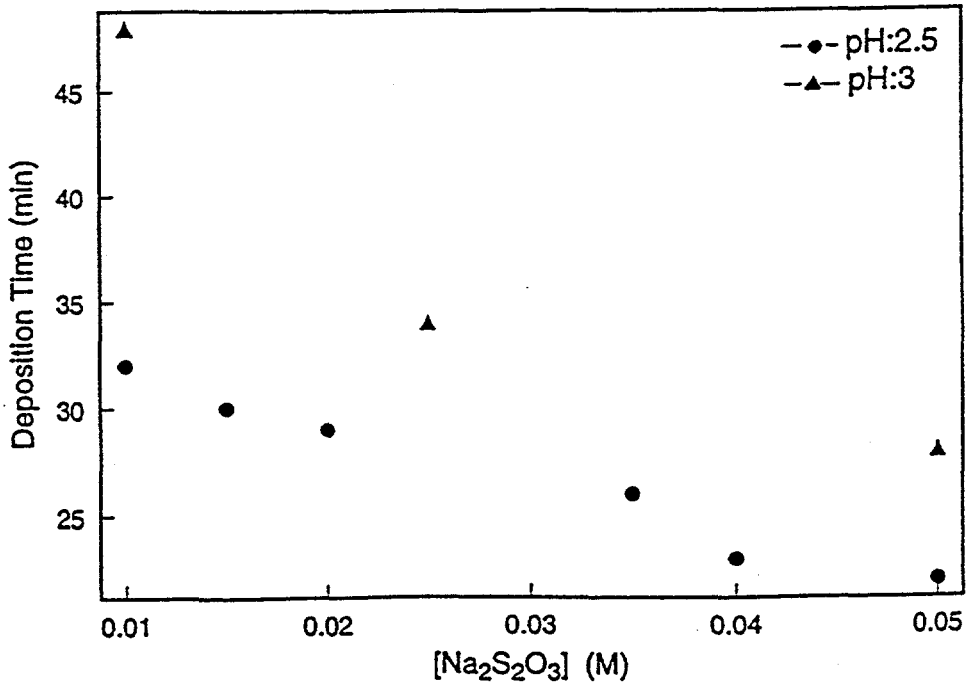

Figure 2. The deposition time required for the passage of 0.16 Coul/cm² charge as a function of the sodium thiosulfate concentration and solution pH. The solution temperature was 90°C. The acid used was HCl.

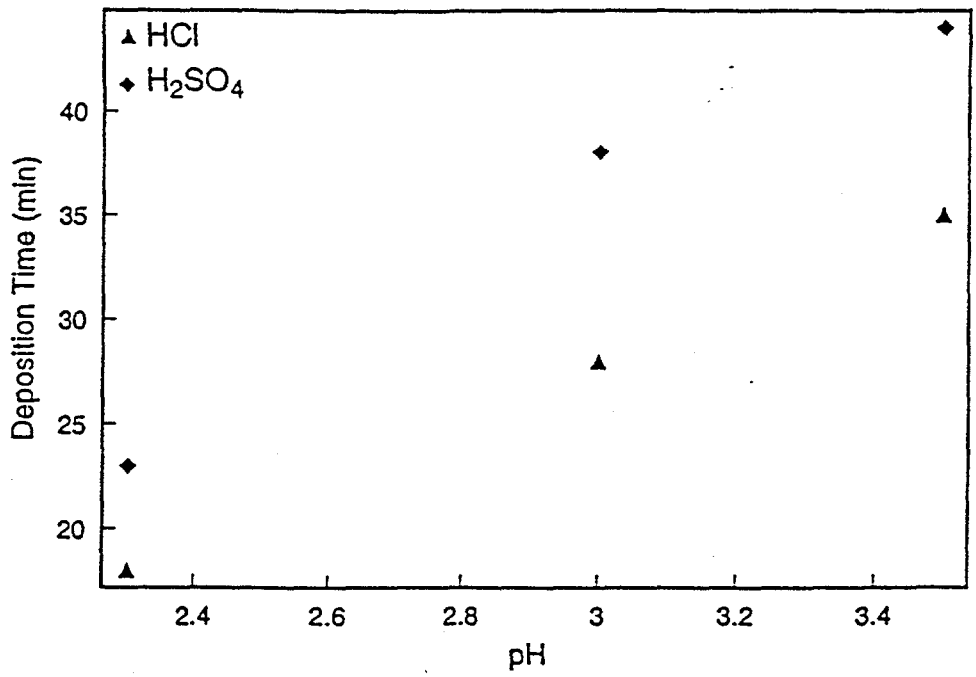

Figure 3. The deposition time required for the passage of 0.16 Coul/cm² charge as a function of solution pH and the acids used. The solution temperature was 90°C.

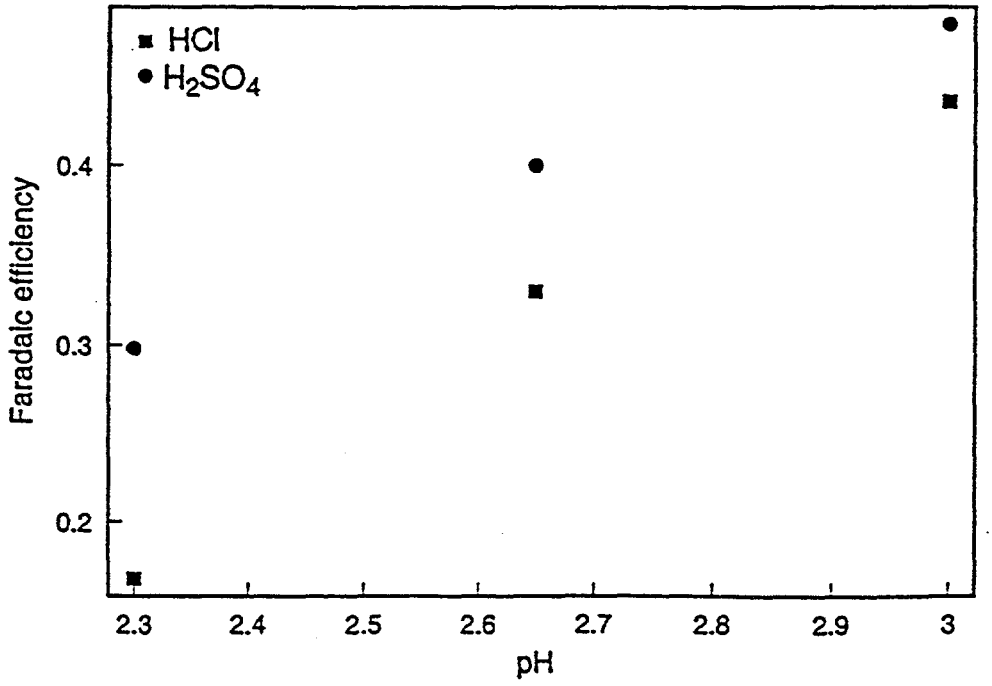

Figure 4. The Faradaic efficiency of the electrodeposition process as a function of solution pH and acids used. The solution temperature was 90°C.

The results are shown in Fig. 4 for deposition in both hydrochloric and sulfuric acid solutions. The Faradaic efficiency is lower at low pH. This is caused presumably by the hydrogen evolution at low pH which contributes to the reduction current. In both cases, the Faradaic efficiency was much lower than unity.

Structural and Compositional Analysis

The morphology of electrodeposited CdS was studied using SEM. The most pronounced difference in film morphology was observed when the temperature of the solution was changed. Fig. 5 shows the SEM images of CdS films electrodeposited under different conditions. Films deposited in a hydrochloric acid solution at 80°C (Fig. 5 a, b) consist of agglomerates of small crystallites. These agglomerates have a rather uniform size of ~0.7 μm and cover the tin oxide substrates uniformly. The crystallites that compose these agglomerates have a typical size of 50 nm. Films deposited at a higher temperature 90°C (Fig. 5 c) are nonuniform with μm-size CdS agglomerates covering only a small portion of the substrates. Films deposited in a sulfuric acid solution at 90°C (Fig. 5 d) are also nonuniform, consisting of agglomerates of varying sizes that cover the substrates completely. Therefore, in terms of film uniformity and cell fabrication, deposition in a hydrochloric acid solution at 80°C is preferred. The improved uniformity can be related to the slow growth rate obtained under such conditions. We have also investigated the effects of substrate materials. Fig. 6 shows the SEM images of films deposited on tin oxide and indium-tin-oxide (ITO) substrates. Films deposited on ITO substrates are much more uniform than films deposited on tin oxide substrates under the same deposition conditions (pH 3.0 and 90°C).

X-ray diffraction was used to characterize the crystalline phase of the electrodeposited CdS. Fig. 7 shows the typical result. The assignment of the peaks is given in the Figure caption. In addition to peaks that may correspond to either cubic or hexagonal CdS (peak 7), we observed several peaks that are present either in hexagonal phase only (peak 1, 3) or in cubic phase only (peak 4), indicating that the electrodeposited CdS is a mixture of hexagonal and cubic phases. This is different from the chemical bath deposited film which, according to our previous study, exhibited only cubic phase.

The composition of the electrodeposited CdS was analyzed using Auger electron spectroscopy. The results are listed in Table 1.

Table 1. Composition of CdS films prepared with electrodeposition.

Samples	Cd (at. %)	S (at. %)	O(at. %)	C (at. %)	Cl(at.%)
ED (pH = 3)	40.6	36.2	3.7	13.7	5.5
ED (pH = 2.65)	44.4	29.7	5.5	11.5	8.4

The ratio of Cd and S concentrations is close to the stoichiometric value for films deposited at a pH of 3.0. At lower pH, the films are more Cd rich.

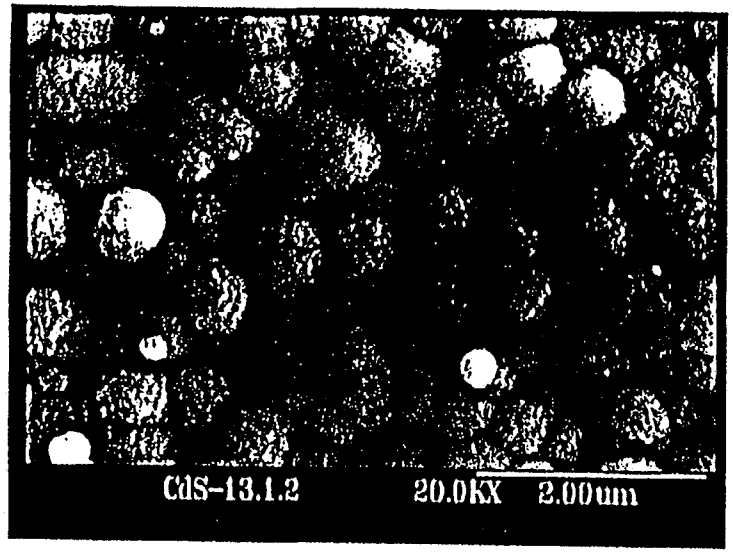

(a)

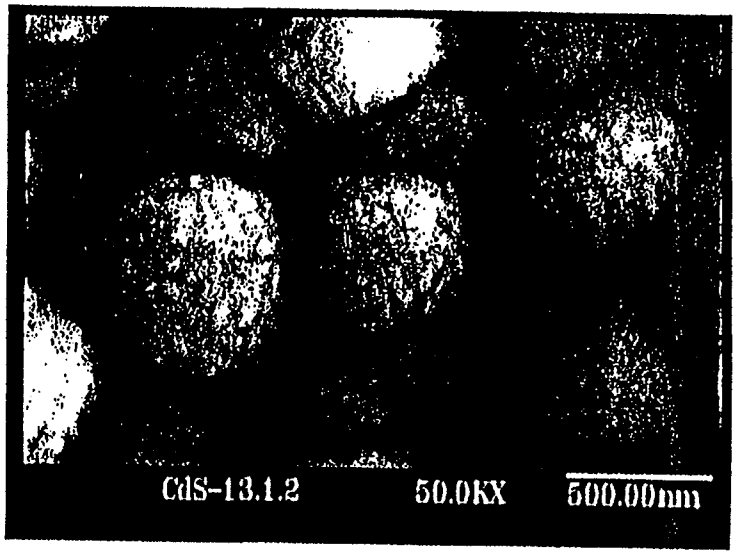

(b)

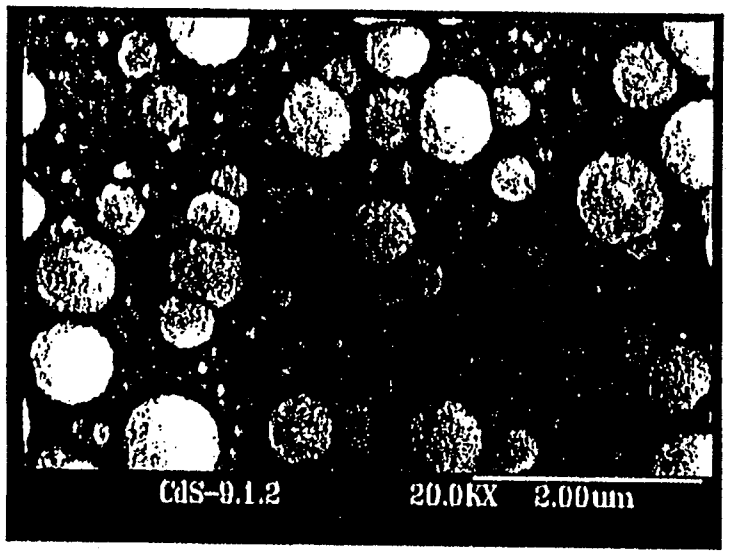

(c)

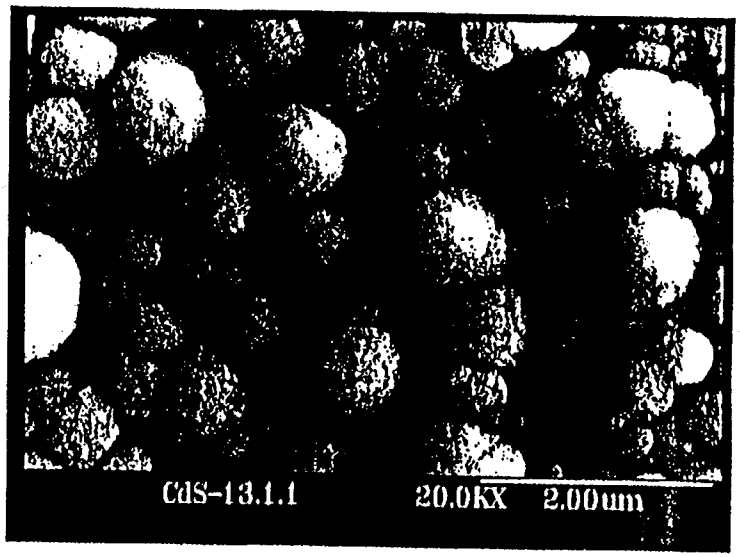

(d)

Figure 5. SEM images of electrodeposited CdS. The solution temperature was 80°C (a, b) and 90°C (c, d). The solution pH was 3.0. The acids used were HCl (a, b, c) and H_2SO_4 (d).

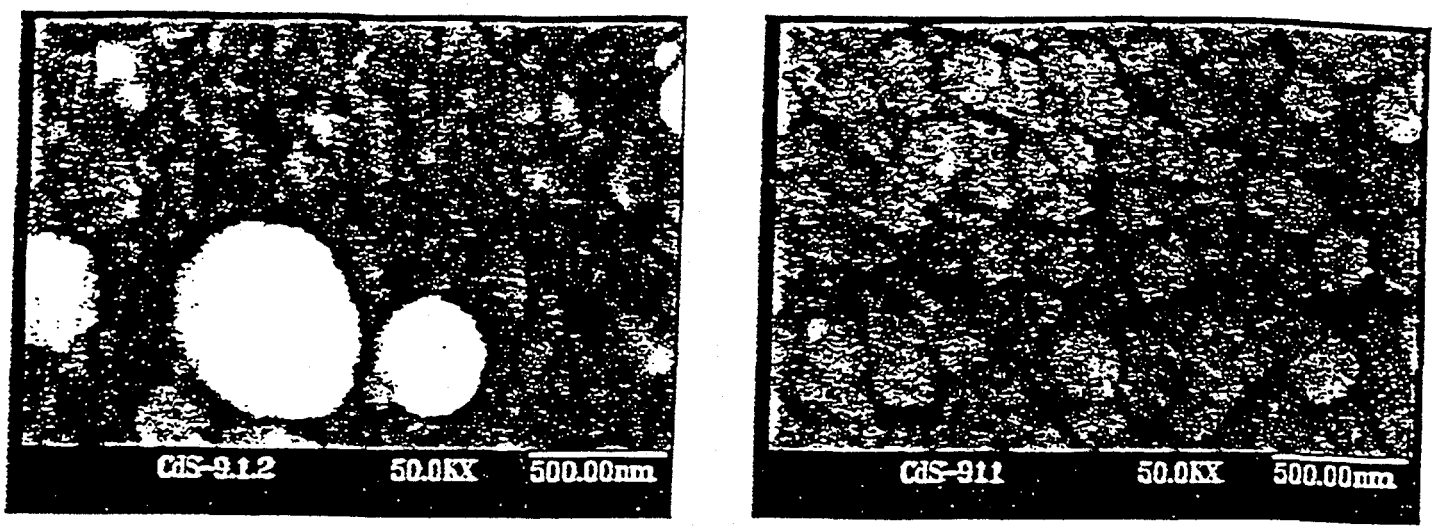

Figure 6. SEM images of CdS films electrodeposited on (a) SnO_2 and (b) ITO substrates.

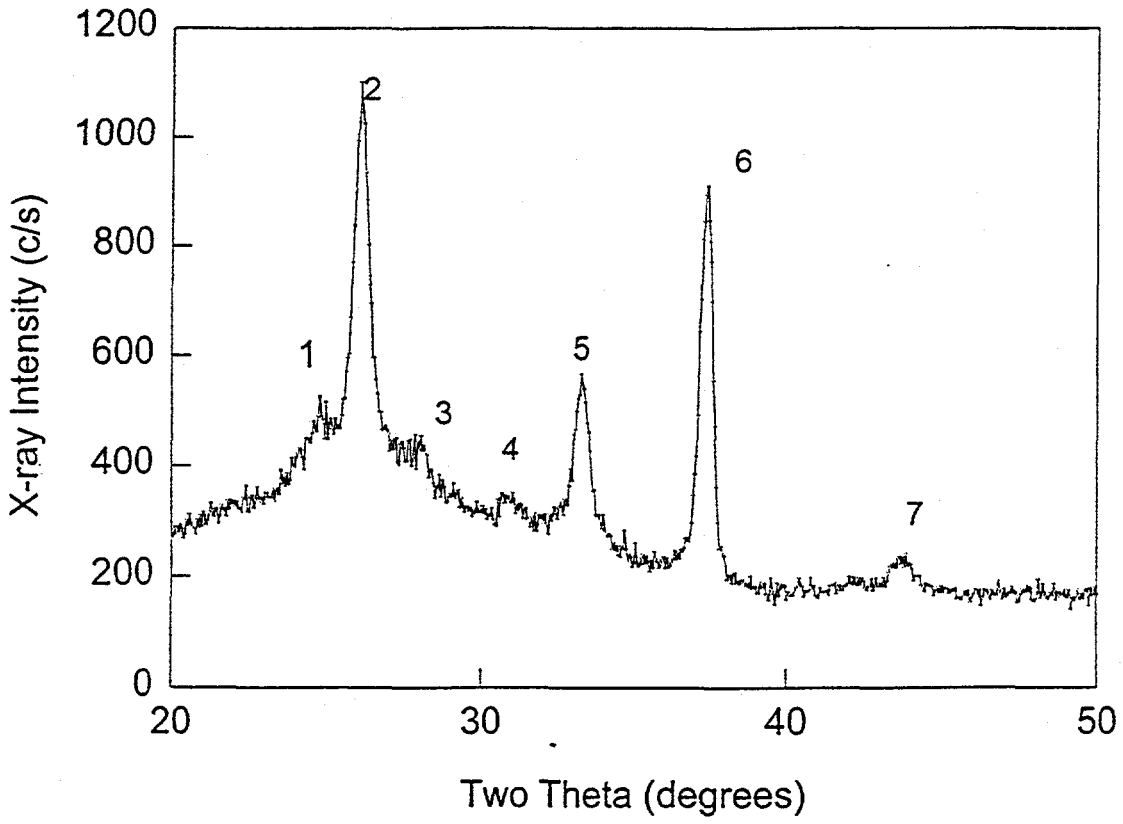

Figure 7. X-ray diffraction of electrodeposited CdS. The peaks are identified as: 1: (100)h; 3: (101)h; 4: (200)c; 7: (110)h or (220)c; Peaks 2, 5, 6 are dominated by SnO_2.

Solar Cell Fabrication Using Electrodeposited CdS

We have prepared CdTe/CdS cells using electrodeposited CdS films. We found that in comparison to the CdS films grown by chemical bath deposition, electrodeposited CdS films have poor adhesion to the tin oxide substrates and flake off easily during CdTe deposition or post-deposition annealing. This problem is especially severe when the CdTe films are thick or when the CdS films are not annealed prior to CdTe deposition. When our standard CdTe/CdS annealing procedure was used, cells made with electrodeposited CdS exhibited a low open-circuit voltage and a low shunt resistance, resulting in low efficiency of the cells (Table 2).

Table 2. Cells made with the standard annealing conditions (annealing of CdTe/CdS films, coated with $CdCl_2$, in air at 410°C for 45 min).

Sample (CdS thickness)	η (%)	V_{oc} (mV)	J_{sc} (mA)	FF (%)	R_s (Ω-cm^2)	R_{sh}
#4 (50 nm)	4.68	371	23.8	52.9	6.54	194
#6 (125 nm)	2.86	298	22.8	42.0	6.93	54.2
#8 (250 nm)	4.67	383	21.7	56.1	5.43	185

We have modified the post-deposition annealing procedure in order to improve the adhesion of CdTe/CdS films formed on electrodeposited CdS. Significant improvement was obtained in terms of V_{oc}, R_{sh}, and the resulting cell efficiency. The open-circuit voltage of 0.65 V and efficiency of 7.7 % obtained with a CdS film thickness of 125 nm are comparable with what we obtained with CBD CdS of a comparable thickness. However, at larger CdS thicknesses, the efficiency of cells fabricated with electrodeposited CdS is much lower than what we obtain typically (upper 700 mV range) with CBD CdS.

Table 3. Cells made with the modified annealing conditions. Sample #5 was not annealed prior to the deposition of the CdTe films. The cells of ED#7 and ED#8 are contacted with ZnTe/Au.

Sample (CdS thickness)	η (%)	V_{oc} (mV)	J_{sc} (mA)	FF (%)	R_s (Ω-cm^2)	R_{sh}
#4 (50 nm)	5.73	433	24.5	53.8	6.94	189
#5 (125 nm)	7.68	654	24.4	48.0	11.3	126
#6 (125 nm)	6.63	503	23.2	56.6	8.28	382
#7 (185 nm)	7.08	612	20.1	57.4	5.55	167
#8 (250 nm)	7.30	518	22.6	62.1	4.74	376

Cells were also made using physical vapor deposited CdTe on electrodeposited CdS. The cell performances are shown in Table 4 for two CdS deposition conditions. The fraction of pinhole area of the CdS is also listed. We can see that the V_{oc} of the cells correlates well with the pinhole density.

Table 4. Cells with physical vapor deposited CdTe on electrodeposited CdS.

CdS deposition condition	η (%)	V_{oc} (mV)	J_{sc} (mA)	FF (%)	R_s (Ω-cm^2)	Fraction of pinhole area
pH=3.00; 90°C	8.7	705	21.4	57.9	6	5×10^{-6}
pH=2.65; 80°C	8.4	629	20.6	64.8	4	3×10^{-5}

3. Effect of Cu Doping on the Properties of ZnTe:Cu Thin Films and the CdS/CdTe/ZnTe Solar Cells

The long-term stability of CdTe thin film solar panels places stringent requirements on the back contact formation techniques. The back contact material we used, thermally evaporated Cu-doped ZnTe, has yielded very low contact resistance (< 0.1 ohm.cm^2) on electrodeposited CdTe thin films and high fill factors (>0.74) in the resulting cells. Because of the well known high diffusivity of Cu in polycrystalline thin films, it is desirable to bring the Cu concentration in these materials to as low a level as possible while still maintaining the performance of the contact. Our previous studies investigated mostly ZnTe films doped with relatively high levels of Cu, between 4 and 10 at. %, with the best device obtained at a Cu concentration of 6 at. %. Hall effect measurement of the films indicated that the acceptor concentration was in the mid 10^{20} cm^{-3} range. This high carrier concentration was more than enough to narrow the ZnTe/metal interface barrier within tunneling distance. It also indicated that only a small fraction of the total Cu concentration was activated. The low doping efficiency of Cu is caused by the combination of several factors: (1) the low processing temperature that was used to limit the Cu diffusion into CdTe; (2) the possible formation of secondary phases between Cu and Te; (3) carrier compensation by structural defects in ZnTe.

We have extended our research by studying ZnTe films doped with low concentrations of Cu. With a lower Cu concentration, the ZnTe:Cu post-deposition annealing temperature can be increased without excessive Cu diffusion into CdTe. The formation of secondary phases will also be reduced. These two factors may lead to an improved Cu doping efficiency in ZnTe, therefore maintaining the quality of the contact. The decreased amount of Cu will certainly be beneficial for the long-term stability of the final devices.

Compositional Analysis

We have studied the ZnTe:Cu film composition as a function of Cu concentration. Electron probe microanalysis was performed on a series of ZnTe:Cu films with nominal Cu concentrations ranging from 1 at. % to 8 at. %. The results are listed in Table 5.

Table 5. Composition of ZnTe doped with different amounts of Cu (measurement performed by Alice Mason of NREL). The film thickness was 0.8 μm.

Nominal Cu (at. %)	Measured Cu (at. %)	Measured Zn (at. %)	Measured Te (at. %)
1.0	0.48	46.39	53.13
2.0	2.35	45.18	52.47
3.0	3.94	45.02	51.03
4.0	6.80	43.84	49.36
6.0	9.79	42.05	48.16
8.0	13.8	39.56	46.68

Except for the lowest Cu concentration, the thickness monitor used for Cu evaporation during ZnTe:Cu deposition underestimated the Cu concentration. The increasingly large deviation of Cu concentration from the nominal concentration suggests that this discrepancy originated from the heating of the quartz crystal by the Cu source during the deposition. A comparison of the concentrations of cations (Zn, Cu) and anions reveals some interesting features (Figure 8): at low Cu concentrations (< 6 at. %), there is a deficiency of cations; at Cu concentrations higher than 6 at. %, the cation concentration exceeds the anion concentration, suggesting that Cu in these films exists mostly in the Cu_2Te-like state. This has implications on the doping mechanism in these films. The cation deficiency at low Cu concentration suggests the existence of Zn vacancies which act as acceptors. The existence of Cu_2Te-like bonding, on the other hand, suggests that most of the Cu atoms are electrically inactive because all the valence electrons are fully coordinated. Finally, we notice that the trend we observed here is consistent with the results reported by Gessert et al. for rf-sputtered Cu-doped ZnTe [3], even though the deposition technique and substrate temperature used were rather different in these two studies.

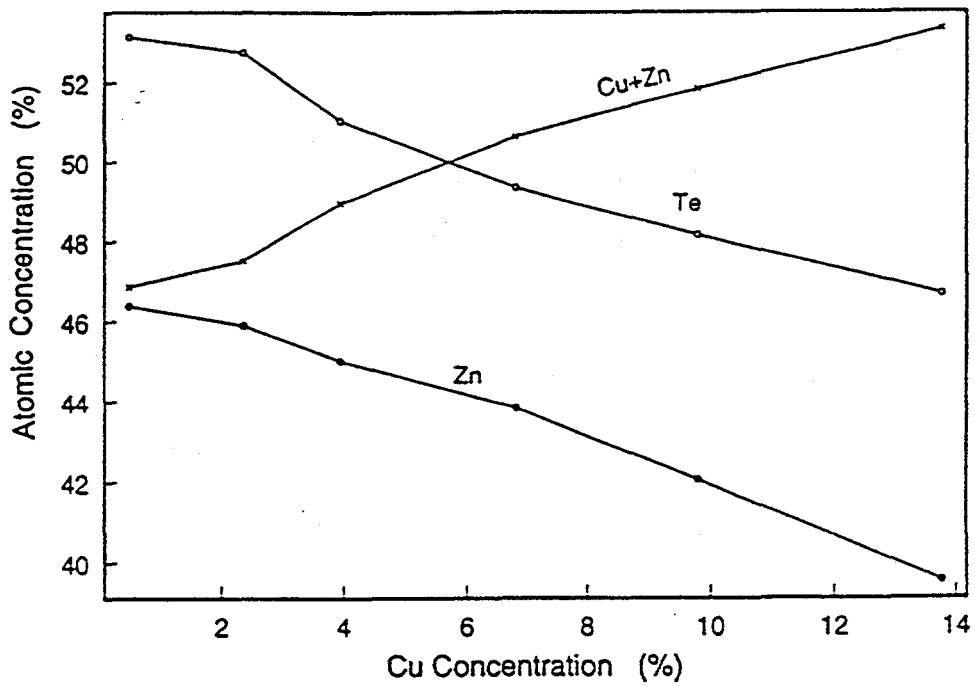

Figure 8. Atomic concentration of Zn, Te, and Zn+Cu as a function of Cu doping concentration in the ZnTe films.

We have performed x-ray photoemission spectroscopy measurements on the ZnTe:Cu films to understand the oxidation states of the Cu dopants. Figure 9 shows the Te 3d and Cu 2p core level photoemission spectra. We do not see any chemical shifts or broadening in either core levels. The binding energy of the Cu 2p lines is in agreement with a Cu^+ assignment.

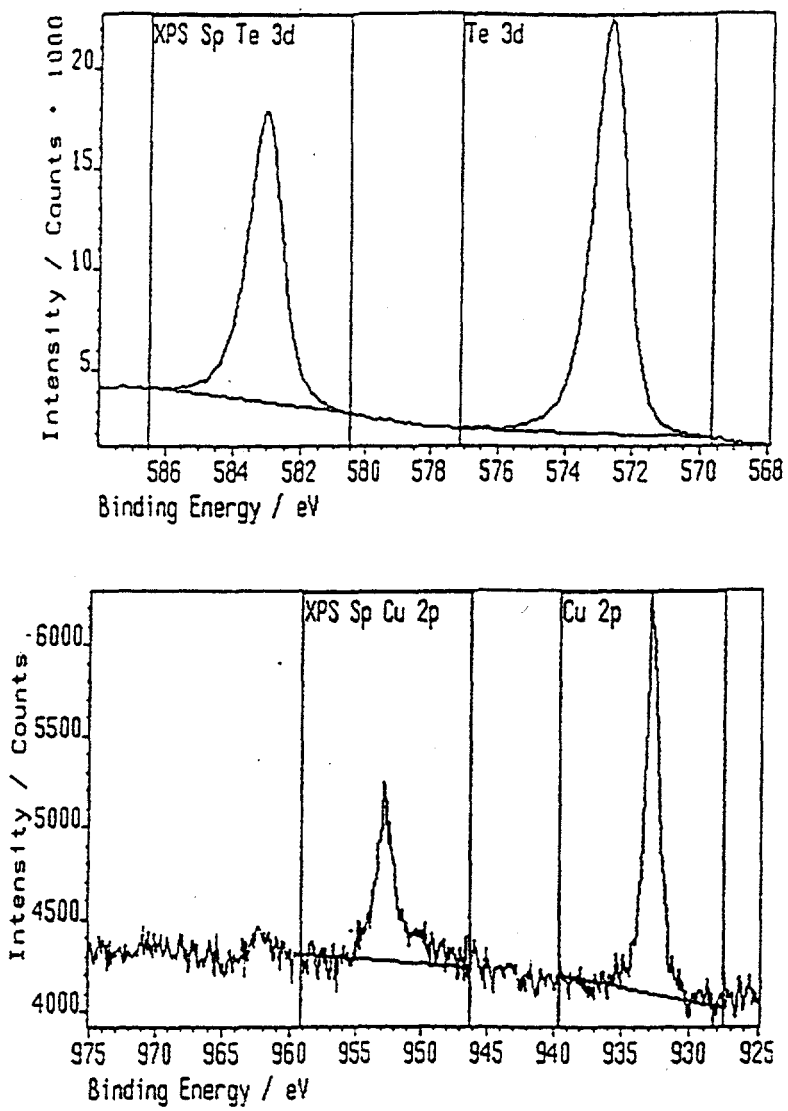

Figure 9. X-ray photoemission spectra of Te 3d and Cu 2p core levels of ZnTe:Cu films.

Hall Effect and Conductivity Measurements

Hall effect measurements were performed on ZnTe films containing various amounts of Cu (1 to 8 at.%) and annealed at different temperatures (250 - 450°C). The results are listed in Table 6.

Table 6. The dependence of film resistivity, sheet resistance, carrier concentration and mobility of ZnTe as a function of Cu concentration and post-deposition annealing temperature. The film thickness was 0.8 μm.

Nominal Cu concentration	Annealing Temperature (°C)	R (Ω/sq)	ρ (Ω-cm)	Mobility ($cm^2/V.s$)	Doping (cm^{-3})
1%	250	4.8×10^{8}	3.8×10^{4}	6.9	2.4×10^{13}
	300	8.0×10^{4}	6.4	6.7	1.5×10^{17}
	350	9.0×10^{3}	0.72	20	4.5×10^{17}
	400	1.5×10^{4}	1.2	21	2.5×10^{17}
	450	1.8×10^{5}	14.0	18	2.6×10^{16}
2%	250	4.7×10^{4}	3.8	0.1	1.4×10^{19}
	300	4.0×10^{3}	0.32	2.8	7.0×10^{18}
	350	1.8×10^{3}	0.14	8.6	5.1×10^{18}
	400	3.6×10^{3}	0.29	13	1.7×10^{18}
	450	6.8×10^{3}	0.55	1.5	7.6×10^{18}
3%	250	1.6×10^{4}	1.3	1.7	2.9×10^{18}
4%	300	3.0×10^{3}	0.24	0.3	7.7×10^{19}
	350	1.2×10^{3}	0.10	1.2	5.4×10^{19}
	450	2.3×10^{4}	1.8	1.9	1.8×10^{18}
6%	250	3.4×10^{4}	2.7	1.1	2.2×10^{18}
	300	150	0.012	1.4	3.8×10^{20}
	350	510	0.041	1.0	1.5×10^{20}
	400	990	0.079	0.6	1.3×10^{20}
	450	690	0.055	2.3	4.9×10^{19}
8%	250	3.3×10^{4}	2.6	1.1	2.2×10^{18}

We can observe several features from Table 6:

1. The lowest resistivity was obtained at an annealing temperature of 350°C. At higher annealing temperatures, the resistivity increases again. In most cases, the increase of resistivity at high annealing temperature was caused by a decrease of carrier concentration.

2. Very high mobility (for polycrystalline p-type ZnTe) was obtained at low (1 to 2 at. %) Cu doping and relatively low annealing temperatures (350°C). With increase in Cu concentration, the mobility decreases, caused possibly by increased scattering by ionized impurities.

3. 2.0 at. % seems to be the lowest Cu doping that can yield a p-type doping concentration of over 10^{18} cm^{-3}. At even lower Cu concentration (0.5 - 1.0 at.%), charge compensation led to very low doping concentration.

4. The highest Cu doping efficiency was obtained at a Cu concentration of 6 at. % for films annealed at high temperatures. For films annealed at a low temperature (250°C), however, the highest doping efficiency was obtained with a Cu concentration of 2 at. %. As shown in the table, the carrier concentration of both 2 at. % and 3 at. % doped films is higher than that of 6 at. % and 8 at. % doped films for the annealing temperature of 250°C. Since low annealing temperature is desired for back contact formation on CdTe, this result suggests that a Cu doping of 2 at. % is preferable.

The conductivities of the films were measured as a function of temperature following annealing under different conditions. A typical result is shown in Figure 10 for a film doped with 2 at. % of Cu. A peak in resistivity was observed in the temperature range between 130 °C and 150 °C, consistent with our previous results obtained with films doped with higher Cu concentration. This peak disappears after 300 °C annealing.

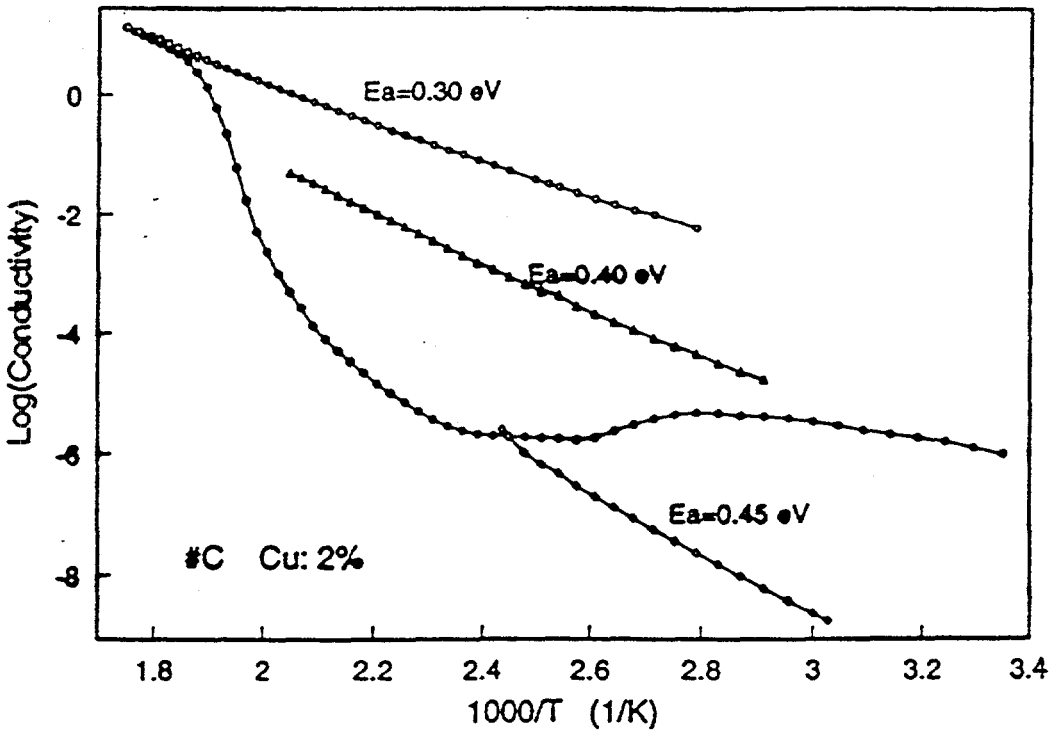

Figure 10. Temperature dependence of dark conductivity of a ZnTe film doped with 2 at. % of Cu.

The activation energy of the conductivity of ZnTe films was deduced from the temperature dependence of dark conductivity between 20–120°C. The results are shown in Table 7. We observe several features:

1. The activation energy of conductivity is rather high (0.6 eV) for the undoped film. The ionization energy of the second level of a Zn-vacancy is a possible interpretation for this activation energy [4].

2. For Cu-doped films, the activation energy is smaller than that of the undoped film and decreases with increasing Cu concentration and annealing temperature. In general, the activation

energy observed was between 0.2 and 0.5 eV. These values correspond well with the ionization energy reported for intrinsic defect levels in ZnTe (0.25 eV, and 0.5 eV) and are higher than the ionization energy of the Cu_{Zn} acceptor level (0.12, 0.15 eV) [5]. This indicates that intrinsic defects (e.g., Zn vacancies) are the dominant acceptors. This can be correlated with the compositional analysis results. As discussed in a previous section, there is a high degree of cation deficiency in low Cu-doped films. This may lead to a high concentration of Zn vacancies. It is possible that the main effect of Cu was to create this cation deficiency rather than acting as an acceptor directly. If this is indeed the case, it may be possible to form Zn-deficient ZnTe films using other mechanisms, thereby eliminating Cu completely.

Table 7. Activation energy of dark conductivity of ZnTe films as a function of Cu concentration and post-deposition annealing temperature.

Cu Concentration	Annealing Temp. (°C)	Activation Energy (eV)
0%	300	0.60
1.0%	145	0.45
	235	0.50
	305	0.41
2.0%	140	0.40
	230	0.45
	300	0.30
3.0%	140	0.42
	225	0.32
	305	0.22
4.5%	145	0.25
	190	0.21
	310	0.22

Optimization of ZnTe contact formation on GPI and SCI CdTe/CdS films

CdS/CdTe solar cells were fabricated with ZnTe films containing low Cu concentrations. Both electrodeposited CdTe films prepared at CSM and films prepared elsewhere (Solar Cells, Inc. and Golden Photon, Inc.) using other techniques were used. Good ohmic contacts were obtained on all films using Cu concentrations as low as 1.0 at. %.

(a) GPI samples

Two types of CdTe/CdS films were provided by GPI: regular and recrystallized (sample

#613). Cu-doped ZnTe was used to make contact on these films and the processing conditions were explored to achieve optimized condition. The parameters we varied include Cu doping concentrations in ZnTe (2.0 to 6.0 at. %), post-deposition annealing temperature (180 to 300°C), and ZnTe:Cu film thickness (50, 100, and 150 nm). Tables 8 and 9 show the cell performance as a function of ZnTe post-deposition temperature and ZnTe:Cu film thickness. (Note that the J_{sc} values listed in Tables 8-12, 15, and 17 are for comparison only and are probably too high.)

Table 8. Performance of cells with different ZnTe:Cu annealing temperatures. The Cu concentration was 2.0 at. %. The thickness of ZnTe was 80 nm.

Annealing Temperature (°C)	η (%)	V_{oc} (mV)	J_{sc} (mA/cm²)	FF (%)	R_s (Ω-cm²)	R_{sh} (Ω-cm²)
240 +190	10.1	780	23.8	54.0	9.2	337
250 + 210	10.2	776	23.9	54.9	6.8	229
270	11.3	781	24.1	59.9	5.7	343

Table 9. Performances of cells fabricated with different ZnTe:Cu thicknesses. The Cu concentration was 4.0 at.%. The annealing temperature was 250°C.

ZnTe Thickness (nm)	η (%)	V_{oc} (mV)	J_{sc} (mA/cm²)	FF (%)	R_s (Ω.cm²)	R_{sh} (Ω.cm²)
50	12.8	799	26.7	59.2	6.4	356
100	13.0	793	27.6	59.3	5.8	344
150	13.3	793	28.9	58.2	6.0	308

So far, the conditions that have yielded the best devices are:

(1) Cu concentration of 2.0 at.%;
(2) Annealing temperature of 270°C;
(3) ZnTe thickness of 100 nm.

Cells made with Sample #613 yielded higher V_{oc} and FF. The cells that were sent to CSU for further characterization had the parameters listed in Table 10. The high series resistance of cells made with regular films seems to originate from bulk resistance of the CdTe film.

In our previous attempts to contact GPI films, we have found that etching of the film prior to contact formation is critical. The bromine-methanol etching we typically use for both our own and SCI films does not work. Therefore, we have coordinated with GPI researchers so that the films were etched at GPI right before we made the ZnTe contact. Another factor that needs to be

considered is the porous film structure and rough surface of GPI samples. It was necessary to ensure that the whole surface was contacted. For this purpose, we used graphite, Ag paint, and an In foil pad to contact the ZnTe:Cu films. However, no effects were apparent.

Table 10. Performance of cells fabricated with ZnTe contacts on GPI films.

Sample	η (%)	V_{oc} (mV)	J_{sc} (mA/cm^2)	FF (%)	R_s (Ω-cm^2)	Rsh (Ω-cm^2)
#613	14.0	816	27.6	62.0	5.2	347
regular	13.0	793	27.6	59.3	5.8	344

(b) SCI samples

Optimization of ZnTe contact on SCI CdTe/CdS films included optimization of Cu concentration and ZnTe post-deposition annealing temperature. The CdTe surface was etched with 0.1% (by volume) bromine-methanol solution for 10 s. The results for various Cu doping concentrations and ZnTe post-deposition annealing temperatures are summarized in Tables 11 and 12.

Table 11. Optimization of Cu concentration in ZnTe for SCI CdTe/CdS films.

Cu Concentration	η (%)	V_{oc} (V)	J_{sc} (mA/cm^2)	FF (%)
1.0%	11.6	0.74	23.8	65.6
2.0%	12.4	0.73	24.8	68.0
3.0%	11.6	0.77	23.3	65.0
4.5%	12.2	0.76	24.0	67.0

Table 12. Cell performance as a function of ZnTe post-deposition annealing temperature. The Cu concentration was 2.0 at.%, ZnTe film thickness was 50 nm.

Annealing Temp. (°C)	η (%)	V_{oc} (mV)	J_{sc} (mA/cm^2)	FF (%)	R_s (Ω-cm^2)
200	1.8	532	9.4	36	20.1
270	13.3	796	23.9	70	4.50
280	12.1	763	23.2	68	4.75
350	7.1	678	20.7	50	18.8

The conditions that yielded best devices are: (a) Cu concentration of 2.0 at.%; (b) annealing temperature of 270 °C.

Mechanism and Stability Studies

In order to probe any possible Cu diffusion from the ZnTe:Cu film into the CdTe, we measured the doping density in the CdTe layer using capacitance-voltage measurements. If Cu does diffuse into the CdTe during the cell fabrication, it would act as an acceptor in the CdTe and higher doping in CdTe would be expected for cells made with ZnTe films containing higher concentrations of Cu or annealed at higher temperatures. As shown in Table 13, there is no obvious correlation between CdTe doping density and Cu doping level in the ZnTe.

Table 13. Effect of Cu concentration in ZnTe on the doping density and depletion width of CdTe deduced from capacitance-voltage measurements of cells.

Cu Concentration in ZnTe	Doping Density in CdTe (cm^{-3})	Depletion Width (μm)
1.0%	4.2×10^{14}	1.8
2.0%	5.0×10^{14}	1.6
3.0%	4.3×10^{14}	1.6
4.5%	2.1×10^{14}	2.3

We also measured the doping density of CdTe as a function of ZnTe post-deposition annealing temperature. As shown in Table 14, we found that higher ZnTe:Cu annealing temperature leads to a higher doping density in CdTe, suggesting Cu diffusion into CdTe layer. We also found that for an annealing temperature of 300 °C, the region closer to the CdTe/ZnTe interface has higher doping density. No such a distinct region was observed in cells fabricated at lower annealing temperatures.

Table 14. CdTe doping density as a function of annealing temperature. The Cu concentration was 2.5 at. %

Sample	Annealing Temperature	Doping in CdTe
44gpi#1	240 °C+ 190 °C	3.9×10^{14}
44gpi#2	250°C+210 °C	5.3×10^{14}
44gpi#3	270 °C	1.0×10^{15}
45gpi#4	300 °C	4.3×10^{15}

We have performed preliminary studies on the stability of ZnTe-contacted cells. Cells were kept in the dark in vacuum for up to 64 hours at 150 °C. I-V and C-V measurements were conducted after 24 and 64 hrs. The results are shown in Table 15.

Table 15. Cell performance after temperature stress (150°C) in the dark. The cells were at open-circuit with no external applied bias.

Annealing time (hr.)	Doping in CdTe (cm^{-3})	η (%)	V_{oc} (mV)	J_{sc} (mA/cm^2)	FF (%)	R_s ($\Omega.cm^2$)	R_{sh} ($\Omega.cm^2$)
0	$7.0x10^{14}$	13.5	789	24.1	70.9	4.02	795
24	$2.1x10^{14}$	11.3	766	24.0	61.4	9.16	586
64	$8.4x10^{13}$	10.1	767	21.1	62.4	10.4	707

After temperature stress at 150 °C, the series resistance increased significantly, leading to decreased FF and degraded cell performances. The doping level of CdTe decreased after the 150 °C stress test. This decreased doping may be caused by the dissociation of Cu_{Cd} acceptors into Cd vacancies and Cu interstitials. A similar behavior has been observed previously by de Nobel in Au doped CdTe [6]. A decrease in hole concentration by nearly one order of magnitude was observed after annealing at 100°C for 1 hour. The decrease was explained in terms of relocation of Au atoms from Cd-substitutional sites to interstitial sites. The interstitial Au atoms act as donors and compensate the Au_{Cd} acceptors, leading to a decreased hole concentration. In our previous study of Cu-doped ZnTe, a similar decrease of conductivity of ZnTe was also observed when the films were annealed in a certain temperature range (between 150° and 170°C).

The changes of CdTe doping and cell performances induced by temperature stress are partially reversible. Brief annealing at 270 °C increased the CdTe doping to $2.7x10^{14}$. The FF of the cells is also partially recovered. A more systematic investigation of temperature stress (at lower temperatures) is in progress. The results will be presented in a future report.

4. Fabrication of CdTe/CdS cells on TiO_2-coated SnO_2 substrates

We participated in team work in exploring the effect of TiO_2 as an intrinsic layer on the SnO_2 substrates. The TiO_2 and SnO_2 films were grown by the Harvard group and the USF group, respectively. The intention was to test if TiO_2 would be more effective in preventing shunting associated with pinholes in CdS. The conduction band offset at the CdS/oxide interface is also expected to be smaller because of the lower electron affinity of TiO_2.

We found that the TiO_2 film is too resistive for the electrodeposition of CdTe. The CdTe films show very poor adhesion and peel off during the deposition or post-deposition annealing. By modifying our annealing procedure, we were able to fabricate cells with limited success. The light I-V curves of cells fabricated with several CdS thicknesses on the TiO_2/SnO_2/glass substrates are shown in Figure 11.

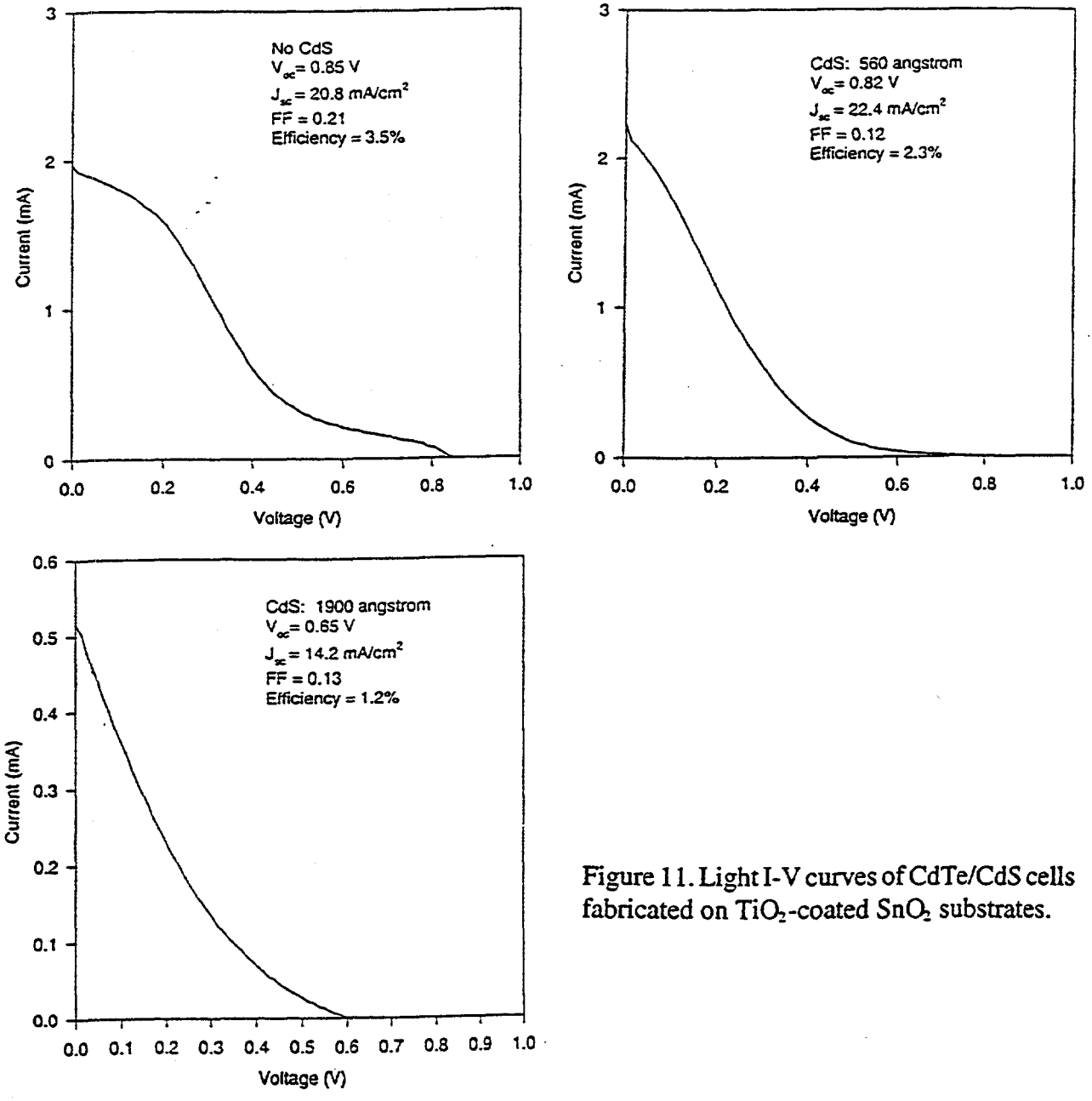

Figure 11. Light I-V curves of CdTe/CdS cells fabricated on TiO_2-coated SnO_2 substrates.

From Figure 11, we notice that cells with no CdS showed the highest efficiency. The V_{oc} value of 0.84 - 0.85 eV is very high for electrodeposited CdTe. The photocurrent is also reasonable. The very poor fill factor was caused by the high resistance of TiO_2. The high V_{oc} and J_{sc} indicate that TiO_2 may be a good candidate for the intrinsic layer between SnO_2 and CdS or as the heterojunction partner with p-type CdTe. The low fill factor may be improved by doping of the TiO_2 film.

Other Team Activities

For the thin CdS team activity, we have prepared CdTe/CdS cells using different CdS thicknesses on SnO_2 substrates provided by USF. The CdS thicknesses, treatment conditions, and the photovoltaic performance of the cells studied are presented in Tables 16 and 17.

Table 16. The CdS thickness and post-deposition treatment conditions

Sample #	CdS thickness	$CdCl_2$-treatment of CdS
A	85 nm	No
B	45 nm	No
C	45 nm	Yes
D	85 nm	Yes

Table 17. The photovoltaic performance of the cells listed in Table 16

Sample	V_{oc} (V)	J_{sc} (mA/cm^2)	FF	Efficiency (%)
A	0.70	24.5	0.59	10.0
B	0.71	25.0	0.59	10.4
C	0.66	25.8	0.48	8.2
D	0.70	26.0	0.59	10.5

Because of the CdS consumption during final annealing of CdTe/CdS films, the final CdS thickness is much smaller than the nominal thickness listed in Table 16. The cells fabricated with very thin and $CdCl_2$-treated CdS showed much lower V_{ox} and fill factor, presumably caused by shunting. This was expected because of the CdS grain growth during $CdCl_2$-treatment which is likely to lead to the formation of pinholes.

6. Summary

During the past year, we have performed systematic studies of the growth and properties of electrodeposition CdS and back contact formation using Cu-doped ZnTe with an emphasis on low Cu concentrations. We have also started to explore the stability of our ZnTe-Cu contacted solar cells.

We have investigated the electrodeposition of CdS and its application in fabricating CdTe/CdS solar cells. The experimental conditions we explored in this study were: pH from 2.0 to 3.0; temperatures of 80° and 90°C; $CdCl_2$ concentration of 0.2 M; deposition potential from -550 to -600 mV vs. Ag/AgCl electrode; $[Na_2S_2O_4]$ concentration between 0.005 and 0.05 M. The deposition rate increases with increase of the thiosulfate concentration and decrease of solution pH. We also observed that the acid used to adjust the pH has a large impact on the deposition rate. The deposition is faster in a hydrochloric acid solution than in a sulfuric acid solution. The surface morphology of electrodeposited CdS thin films was investigated using scanning electron microscopy. The most pronounced difference in film morphology was observed for different solution temperatures. Films deposited in a hydrochloric acid solution at 80°C consist of agglomerates of small crystallites. These agglomerates have a rather uniform size of ~ 0.7 μm and cover the tin oxide substrates uniformly. Films deposited at a higher temperature of 90°C are nonuniform with μm-size CdS agglomerates covering only a small portion of the substrates. Therefore, in terms of film uniformity and cell fabrication, deposition in a hydrochloric acid solution at 80°C is preferred. The improved uniformity can be related to the slow growth rate obtained under such conditions. CdTe/CdS cells were prepared using electrodeposited and physical vapor deposited CdTe on electrodeposited CdS. Moderate cell efficiencies were obtained in the preliminary study.

We have extended our previous research of ZnTe:Cu films by investigating films doped with low Cu concentrations (<5.0 at. %). The low Cu concentration enabled us to increase the ZnTe:Cu post-annealing temperature without causing excessive Cu diffusion into CdTe or formation of secondary phases. The effects of Cu doping concentration and post-deposition annealing temperature on the structural, compositional, and electrical properties of ZnTe were studied systematically using x-ray diffraction, atomic force microscopy, electron microprobe, Hall effect and conductivity measurements. XRD measurements indicated that the crystalline phase of as-deposited and low-temperature annealed ZnTe films is dependent on Cu doping concentration. Low-Cu-doped films exhibited zincblend phase, whereas high-Cu-doped films showed wurtzite phase. After annealing at high temperature (≥350°C), all films exhibited zincblend structure. Electron probe microanalysis revealed a deficiency of cations in low-Cu-doped films and an excess of cations in high-Cu-doped films. Hall effect measurements revealed a dependence of hole mobility on Cu doping concentration with the highest mobility (20 cm^2/Vs) obtained at a low Cu concentration of 2 at.% and relatively low annealing temperatures. Studies of the activation energy of dark conductivity suggested that intrinsic defects (e.g., Zn vacancies) are the dominant acceptors for Cu concentrations lower than 4.5 at.%. Finally, ZnTe films with Cu concentrations as low as 1 at. % were used successfully as a back contact layer in CdTe based solar cells. Fill factors over 0.70 were obtained using films of low Cu doping.

7. Acknowledgements

We thank the scientists at the National Renewable Energy laboratory (NREL) for various measurements, especially David Niles for XPS measurements, Alice Mason for electron probe microanalysis, and Helio Moutinho for atomic force microscopy measurements. We thank the NREL CdTe team members: Peter Sheldon, David Albin, Xiaonan Li, Tim Gessert, and Doug Rose for many helpful discussions and experimental help. We thank Brian McCandless of the Institute of Energy Conversion, the University of Delaware for pinhole density survey and cell fabrication on electrodeposited CdS films and high temperature treatment of electrodeposited CdTe films. The investigation of the effects of CdS film thickness and TiO_2 coating on cell performances and back contact optimization on SCI and GPI films were part of a coordinated effort of the Thin Film Photovoltaic Partnership team. Chris Ferekides of the University of South Florida provided SnO_2-coated glass substrates. Roy Gordan of Harvard University deposited the TiO_2 layer. Solar Cells, Inc. and Golden Photon, Inc. provided CdTe/CdS films prepared by sublimation and spray pyrolysis. Finally, we thank Kenneth Zweibel and Bolko von Roedern of NREL for helpful discussions and encouragement.

8. References

1. J. Tang, D. Mao, L. Feng, W. Song, and J.U. Trefny, *Proc. 25th IEEE Photovoltaic Specialists Conference*, 1996, pp. 925-928.

2. J. Tang, L. Feng, D. Mao, W. Song, Y. Zhu, and J.U. Trefny, *Mater. Res. Soc. Symp. Proc.* **426**, 1996, pp. 355-360

3. T.A. Gessert, A.R. Mason, R.C. Reedy, R. Matson, T.J. Coutts, and P. Sheldon, *J. Electronic Materials*, Vol. 24, p.1443 (1995); T.A. Gessert, A.R. Mason, P. Sheldon, A.B. Swartzlander, D. Niles, and T.J. Coutts, *J. Vac. Sci. & Technol.* Vol. A14, p.806 (1996).

4. T.L. Larsen, C.F. Varotto, and D.A. Stevenson, *J. Appl. Phys.* **43**, 172 (1972).

5. H. Tubota, *Jap. J. Appl. Phys.* **2**, 259 (1963); M. Aven, and B. Segall, *Phys. Rev.* **130**, 81 (1963).

6. D. de Nobel, *Phillips Res. Rep.* **14**, 430 (1959)

9. Appendices

9.1. Personnel

Many individuals contributed to this work. Their names, titles, and representative responsibilities are summarized below.

John U. Trefny, Professor of Physics: Project Coordinator.

Duli Mao, Research Assistant Professor: Photovoltaic Development.

Don L. Williamson, Professor of Physics: Structural Properties of Materials.

Reuben T. Collins, Professor of Physics: Electronic and Optical Properties of Semiconductors.

Thomas E. Furtak, Professor of Physics: Electrochemistry, Optical Properties.

Timothy R. Ohno, Assistant Professor of Physics: Surface Physics.

Yuming Zhu, Graduate Research Assistant: CdS Chemical Bath Deposition.

Wenjie Song, Graduate Research Assistant: CdTe Electrodeposition and Cell Optimization.

Jian Tang, Graduate Research Assistant: ZnTe Back Contact, Cell Fabrication, and Stability.

Figen Kadirgan, Visiting Professor: Electrodeposition of CdS.

Sana Kutun, Visiting Graduate Student: Electrodeposition of CdS.

M. Hasan Aslan, Graduate Student: Photoluminescence.

Ahmed Alkaoud, Graduate Student: Transparent Conducting Oxide.

Troy Berens, Graduate Student: Copper Indium Diselenide Thin Film Solar Cells.

Ahmed Balcioglu, Graduate Student: Surface Analysis and Deep Level Transient Spectroscopy.

9.2. Laboratory Improvements

1. A major laboratory renovation project was finished during the past year. This laboratory renovation project was supported by the Infrastructure Program of National Science Foundation with matching funds from the School of Mines. The total investment of NSF and CSM in this new facility exceeded $800,000 and provided a new 2,200 sq. ft. thin film processing laboratory with 3 more filtered fume hoods, a class-1,000 clean room, ample lab space, and other hardware related to the safety of staff members and students. During the renovation, efforts were made to minimize the disruption of the construction work to the CdTe project.

2. A proposal for the "Acquisition of Characterization Instrumentation for Advanced Materials Research" to the Infrastructure (Instrumentation) Program of NSF was granted. This allowed us to acquire 4 pieces of equipment that are critically important for our thin film research: a Tencor P-10 surface profiler with three-dimensional imaging capability, a Cary 5G UV-Vis-NIR spectrophotometer with diffuse reflection accessory, a variable temperature Hall effect measurement station, and a three-wavelength (633, 830, 1300 nm) ellipsometer. In addition, Professor Ohno has acquired an x-ray photoemission spectroscopy system, also sponsored by the Infrastructure (Instrumentation) Program of NSF. These new instruments have all arrived and are functioning. This is expected to greatly facilitate our CdTe thin films research.

For the infrastructure projects listed above, the Colorado School of Mines has provided about $800,000 in matching funds, demonstrating clearly its strong commitment to thin films and photovoltaics research.

9.3. Publications

"The Structural, Optical, and Electrical Properties of Vacuum Evaporated Cu-doped ZnTe Polycrystalline Thin Films", L.H. Feng, D. Mao, J. Tang, R. Collins, and J.U. Trefny, *J. Electron. Materials* **25**,1433 (1996).

"Effect of Annealing on Microstructure, Residual Stress, and Photovoltaic Characteristics of Electrodeposited CdTe Films", B. Qi, D. Kim, D.L. Williamson, and J.U. Trefny, *J. of Electrochem. Soc.* **143,** 517 (1996).

"Effect of $CdCl_2$ Treatment of CdS Films on CdTe/CdS Solar Cells", W. Song, D. Mao, L. Feng, Y. Zhu, M.H. Aslan, R.T. Collins, and J.U. Trefny, *Mater. Res. Soc. Symp. Proc.* **426**, 1996, pp. 331-336.

"Study of ZnTe:Cu Back Contacts on CdTe/CdS Thin Film Solar Cells", J. Tang, L. Feng, D. Mao, W. Song, Y. Zhu, and J.U. Trefny, *Mater. Res. Soc. Symp. Proc.* **426**, 1996, pp. 355-360.

"Chemical Bath Deposition of CdS Thin Films: Growth and Structural Studies", Y. Zhu, D. Mao, D.L. Williamson, and J.U. Trefny, *Mater. Res. Soc. Symp. Proc.* **426**, 1996, pp. 227-232.

"Fabrication of CdTe Thin Film Solar Cells Using Electrodeposition", W. Song, D. Mao, Y. Zhu, J. Tang, and J.U. Trefny, *Proc. 25th IEEE Photovoltaic Specialists Conference,* 1996, pp. 873-876.

"The Properties and Optimization of ZnTe:Cu Back Contacts on CdTe/CdS Thin Film Solar Cells", J. Tang, D. Mao, L. Feng, W. Song, and J.U. Trefny, *Proc. 25th IEEE Photovoltaic Specialists Conference,* 1996, pp. 925-928.

"Effect of Cu Doping on the Properties of ZnTe:Cu Thin Films and CdS/CdTe/ZnTe Solar Cells", J. Tang, D. Mao, and J. U. Trefny, *Proc. 14th NREL Photovoltaic Program Review Meeting,* 1996, pp.639-646.

REPORT DOCUMENTATION PAGE

Form Approved
OMB NO. 0704-0188

1. AGENCY USE ONLY (Leave blank)	2. REPORT DATE	3. REPORT TYPE AND DATES COVERED
	January 1998	Annual Technical Report

4. TITLE AND SUBTITLE

Polycrystalline Thin-Film Cadmium Telluride Solar Cells Fabricated by Electrodeposition; Annual Technical Report

5. FUNDING NUMBERS

C: XAF-5-14142-11
TA: PV804401

6. AUTHOR(S)

J.U. Trefny and D. Mao

7. PERFORMING ORGANIZATION NAME(S) AND ADDRESS(ES)

Department of Physics
Colorado School of Mines
Golden, Colorado

8. PERFORMING ORGANIZATION REPORT NUMBER

9. SPONSORING/MONITORING AGENCY NAME(S) AND ADDRESS(ES)

National Renewable Energy Laboratory
1617 Cole Blvd.
Golden, CO 80401-3393

10. SPONSORING/MONITORING AGENCY REPORT NUMBER

SR-520-23994

11. SUPPLEMENTARY NOTES

NREL Technical Monitor: B. von Roedern

12a. DISTRIBUTION/AVAILABILITY STATEMENT

12b. DISTRIBUTION CODE

UC-1263

13. ABSTRACT *(Maximum 200 words)*

During the past year, Colorado School of Mines (CSM) researchers performed systematic studies of the growth and properties of electrodeposition CdS and back-contact formation using Cu-doped ZnTe, with an emphasis on low Cu concentrations. CSM also started to explore the stability of its ZnTe-Cu contacted CdTe solar cells. Researchers investigated the electrodeposition of CdS and its application in fabricating CdTe/CdS solar cells. The experimental conditions they explored in this study were pH from 2.0 to 3.0; temperatures of 80° and 90°C; $CdCl_2$ concentration of 0.2 M; deposition potential from -550 to -600 mV vs. Ag/AgCl electrode; $[Na_2S_2O_4]$ concentration between 0.005 and 0.05 M. The deposition rate increases with increase of the thiosulfate concentration and decrease of solution pH. Researchers also extended their previous research of ZnTe:Cu films by investigating films doped with low Cu concentrations (<5 at. %). The low Cu concentration enabled us to increase the ZnTe:Cu post-annealing temperature without causing excessive Cu diffusion into CdTe or formation of secondary phases. The effects of Cu doping concentration and post-deposition annealing temperature on the structural, compositional, and electrical properties of ZnTe were studied systematically using X-ray diffraction, atomic force microscopy, electron microprobe, Hall effect, and conductivity measurements.

14. SUBJECT TERMS

photovoltaics ; polycrystalline thin films ; cadmium telluride ; electrodeposition ; cell fabrication ; CdS/CdTe solar cells ; module energy rating

15. NUMBER OF PAGES

37

16. PRICE CODE

17. SECURITY CLASSIFICATION OF REPORT	18. SECURITY CLASSIFICATION OF THIS PAGE	19. SECURITY CLASSIFICATION OF ABSTRACT	20. LIMITATION OF ABSTRACT
Unclassified	Unclassified	Unclassified	UL